Commun Nonlinear Sci Numer Simulat 55 (2018) 93–104

Contents lists available at ScienceDirect

Commun Nonlinear Sci Numer Simulat

journal homepage: www.elsevier.com/locate/cnsns

Research paper

Time-splitting combined with exponential wave integrator fourier pseudospectral method for Schrödinger–Boussinesq system☆

Feng Liao, Luming Zhang*, Shanshan Wang

College of Science, Nanjing University of Aeronautics and Astronautics, Nanjing 211106, China

ARTICLE INFO

Article history:
Received 7 January 2017
Revised 10 May 2017
Accepted 22 June 2017
Available online 23 June 2017

Keywords:
Schrödinger–Boussinesq system
Time-splitting
Pseudospectral
Fast Fourier transform

ABSTRACT

In this article, we formulate an efficient and accurate numerical method for approximations of the coupled Schrödinger–Boussinesq (SBq) system. The main features of our method are based on: (i) the applications of a time-splitting Fourier spectral method for Schrödinger-like equation in SBq system, (ii) the utilizations of exponential wave integrator Fourier pseudospectral for spatial derivatives in the Boussinesq-like equation. The scheme is fully explicit and efficient due to fast Fourier transform. The numerical examples are presented to show the efficiency and accuracy of our method.

1. Introduction

The coupled Schrödinger–Boussinesq (SBq) system is used to describe various physical processes in the field of laser and plasma, such as the interaction of long waves with short wave packets in nonlinear dispersive media and diatomic lattice system [40], and the dynamics behavior of Langmuir soliton formation [32]:

$$\begin{cases} iu_t + \gamma\Delta u = \xi uv, & \mathbf{x} \in \mathbb{R}^d, \\ v_{tt} = \Delta v - \alpha\Delta^2 v + \Delta(f(v) + \omega|u|^2), & \mathbf{x} \in \mathbb{R}^d, \end{cases} \tag{1.1}$$

where the complex function u represents the electric field of Langmuir oscillations while the real function v describes the low-frequency density perturbation, γ, ξ, ω and $\alpha > 0$ are real constants, $f(\cdot)$ is a sufficiently smooth function with $f(0) = 0$.

The SBq system preserves the total mass

$$Q(t) = \int_{\mathbb{R}^d} |u(\mathbf{x}, t)|^2 d\mathbf{x} = Q(0) \tag{1.2}$$

☆ The work of F. Liao is supported by Jiangsu Innovation Program for Graduate Education (KYZZ160161) and the National Natural Science Foundation of China (11571181). The work of S.S.Wang is supported by the Fundamental Research Funds for the Central Universities (NS2015075).

* Corresponding author.
E-mail addresses: wawjd3kwcom@163.com (F. Liao), zhanglm@nuaa.edu.cn (L. Zhang), wangss@nuaa.edu.cn (S. Wang).

http://dx.doi.org/10.1016/j.cnsns.2017.06.033
1007-5704/

and total energy

$$E(t) = \int_{\mathbb{R}^d} \Big[v^2(\mathbf{x},t) + |\nabla\phi(\mathbf{x},t)|^2 + \frac{2\omega\gamma}{\xi}|\nabla u(\mathbf{x},t)|^2 + \alpha|\nabla v(\mathbf{x},t)|^2 + 2F(v(\mathbf{x},t)) + 2\omega v(\mathbf{x},t)|u(\mathbf{x},t)|^2 \Big] d\mathbf{x} = E(0), \tag{1.3}$$

where $\phi(\mathbf{x}, t)$ is defined via $\Delta\phi = v_t$ with $\lim_{|\mathbf{x}|\to\infty}\phi(\mathbf{x},t) = 0$ for $t \geq 0$ and $F(v)$ is a primitive function of $f(v)$. When $f(\cdot) \equiv 0$ and $\alpha = 0$, the system of SBq degenerates into the well-known Zakharov system

$$\begin{cases} iu_t + \gamma\Delta u = \xi uv, & \mathbf{x} \in \mathbb{R}^d, \\ v_{tt} = \Delta v + \omega\Delta(|u|^2), & \mathbf{x} \in \mathbb{R}^d, \end{cases}$$

which has been first derived by Zakharov [42] to describe the interaction between Langmuir (dispersive) and ion acoustic (approximately non-dispersive) waves in plasma. Up to now, the numerical studies of Zakharov system are very rich, one could reference [9,11,26,27,39] (and references therein) for more details.

In the literature, many works have been concentrated on the theoretical studies of this problem. Guo [19] investigated the existence and uniqueness of the global solutions with initial value problem or periodic boundary value problem. Guo and Chen [20] considered the global existence and long time behavior of SBq system with initial boundary condition. In [15], the authors analyzed the local and global well-posedness of the periodic boundary value problem. Li and Chen [29] examined the initial boundary value problem of dissipative SBq system and proved the existence of global attractors. The attractor and its regularity for damped SBq system was studied in [21]. While, in [22], Guo and Du discussed the existence and uniqueness of periodic strong solutions for the same problem. During the past several years, there are several papers for finding the solitary-wave solutions of SBq system, readers can refer to the relevant works in [10,24,28,31,32,41] (and references therein) for more details.

Tracing the literature regarding the studies of SBq system, the numerical methods proposed in the literature are limited. Guo and Chen [23] formulated Galerkin–Fourier methods to study SBq system. In [1,46], finite element methods (FEM) were proposed and analyzed. Bai and Wang [2] investigated a time-splitting Fourier spectral method for SBq system. Huang et al. [25] considered a conservative multisymplectic scheme based on center discrete method. Zhang et al. [43] constructed a conservative finite difference scheme with order $O(\tau^2 + h^2)$. Recently, we developed two conservative compact finite difference schemes in [30], the convergence and stability were analyzed by means of discrete energy methods. However, these methods are fully implicit and at each time step, a nonlinear problem has to be solved very accurately which is quite time-consuming. The main purpose of this paper is to construct a time-splitting exponential wave integrator Fourier pseudospectral (TS-EWI-FP) method for SBq system.

The basic idea of time-splitting method is to decompose the original problem into sequential subproblems which are simpler and easier to implement than the original problem. In the past several decades, time-splitting method is widely used to compute the nonlinear Schrödinger equation (NLS). In [35], Wang investigated a time-splitting finite difference (TSFD) method for various versions of NLS. To improve the accuracy of TSFD, Dehghan and Taleei [12] constructed a compact TSFD, which was proved to be unconditionally stable and preserve some invariant properties. Subsequently, Taleei and Dehghan [34] employed time-splitting combined with multi-domain Chebyshev pseudospectral method to solve NLS. Comparing with the single-domain method, multi-domain method can reduce memory requirements and allow for the best use of parallel computations. In [36], Wang and Zhang combined orthogonal spline collocation (OSC) approach with time-splitting method to solve NLS in different space dimensions. Later, Wang et al. [37] proposed various time-splitting Fourier pseudospectral methods for N-coupled NLS. Bai and Zhang [3] formulated time-splitting quadratic B-spline finite element method for the coupled Schrödinger-KDV equations. To summarize, time-splitting method is easy to combined with popular numerical methods such as finite difference method, finite element method, pseudospectral method, OSC method and so on. Thus, time-splitting method has evolved as a valuable technique for the numerical approximation of partial differential equations. For more works the interested reader can see [7–9,26,27,33,38] and the references therein.

The exponential wave integrator (EWI) is fully explicit and very efficient due to fast Fourier transform (FFT), thus, the EWI method has been widely used in the solving PDE numerically. Bao and Dong [4] investigated a Gautschi-type exponential integrator Fourier pseudospectral method for Klein–Gordon (KG) equation. A trigonometric integrator Fourier pseudospectral (TIFP) method for solving the N-coupled KG equations was formulated in [13], but which was lack of rigorous stability and convergence analysis. Subsequently, the author developed a modified TIFP method for the same problem, and the rigorous error estimates were established in [14]. In [5], Bao et al. derived an efficient and accurate three-level scheme for the Klein–Gordon–Zakharov (KGZ) system based on Gaustchi-type exponential wave integrator sine pseudospectral (EWI-SP) method. Recently, Zhao [44] presented an EWI-SP method based on Deuflhard-type quadrature for KGZ system, and rigorous error estimates were established for the method with no CFL-type conditions. Readers can refer to the works [6,16–18,45] for more relevant references.

The outline of this paper is organized as follows. In Section 2, we propose EWI method based on Gautschi-type quadrature and Fourier pseudospectral discretization for solving Boussinesq-like equation, then we present the time-splitting Fourier spectral discretization of Schrödinger-like equation. Enlightened by TS-EWI-FP method for 1D SBq system, we provide TS-EWI-FP method with more details for 2D SBq system in Section 3. In Section 4, we investigate the accuracy of

TS-EWI-FP for SBq system with solitary-wave solutions, and apply it to study the dynamics of SBq and Zakharov system in 2D. Finally, some conclusions are drawn in Section 5.

2. Numerical methods for SBq system

In this section, we formulate an efficient and accurate numerical method for SBq system. For simplicity of notation, we introduce the method for SBq system with periodic boundary conditions in one space dimension ($d = 1$). Generalizations to ($d > 1$) are straightforward for tensor product grids and the results remain valid without modification. In this paper, we truncate the whole space problem (1.1) onto a finite interval $\Omega = (a, b)$. For $d = 1$, the problem collapses to

$$iu_t + \gamma u_{xx} = \xi uv, x \in \Omega, t > 0, \tag{2.1}$$

$$v_{tt} = v_{xx} - \alpha v_{xxxx} + (f(v))_{xx} + \omega(|u|^2)_{xx}, x \in \Omega, t > 0, \tag{2.2}$$

$$u(a,t) = u(b,t), v(a,t) = v(b,t), v_x(a,t) = v_x(b,t), t \geq 0, \tag{2.3}$$

$$u(x,0) = u^{(0)}(x), v(x,0) = v^{(0)}(x), v_t(x,0) = v^{(1)}(x), x \in \Omega, \tag{2.4}$$

where $u^{(0)}(x)$, $v^{(0)}(x)$ and $v^{(1)}(x)$ are periodic functions with the period $b - a$.

2.1. Exponential wave integrator Fourier pseudospectral method for Boussinesq-like equation

We formulate an exponential wave integrator Fourier pseudospectral (EWI-FP) discretization for Boussinesq-like equation in (2.2), which applies the Fourier pseudospectral discretization to spatial derivatives followed by using EWI for temporal discretization in phase space.

Choose a mesh size $h := (b - a)/N$ with N an even positive integer, time step τ, and denote grid points with coordinates $(x_j, t_n) := (a + jh, n\tau)$ for $j = 0, 1, \ldots, N$ and $n \geq 0$. Denote

$$X_N := span\left\{ \Phi_l(x) = e^{i\mu_l(x-a)} : x \in \overline{\Omega}, \mu_l = \frac{2\pi l}{b-a}, -N/2 \leq l \leq N/2 - 1 \right\}$$

and

$$Y_N := \left\{ u = (u_0, u_1, \ldots, u_N) \in \mathbb{C}^{N+1} : u_0 = u_N \right\}.$$

Define projection operator $\mathcal{P}_N : Y = \{u(x) \in L^2(\Omega) : u(a) = u(b)\} \to X_N$ and interpolation operator $\mathcal{I}_N : Y_N \to X_N$ as follows

$$(\mathcal{P}_N u)(x) = \sum_{l=-N/2}^{N/2-1} \hat{u}_l \Phi_l(x), (\mathcal{I}_N u)(x) = \sum_{l=-N/2}^{N/2-1} \tilde{u}_l \Phi_l(x), x \in \overline{\Omega} \tag{2.5}$$

with

$$\hat{u}_l = \frac{1}{b-a} \int_a^b u(x) e^{-i\mu_l(x-a)} dx, \tilde{u}_l = \frac{1}{N} \sum_{j=0}^{N-1} u_j e^{-i\mu_l(x_j - a)}. \tag{2.6}$$

Obviously, we have

$$\|(\mathcal{I}_N u)(x)\|_{L^2}^2 = (b-a) \sum_{l=-N/2}^{N/2-1} |\tilde{u}_l|^2, \int_a^b (\mathcal{I}_N u)(x) dx = (b-a)\tilde{u}_0, \tag{2.7}$$

where $\|u\|_{L^2}^2 = \int_a^b |u|^2 dx$ for $u \in L^2(\Omega)$. Define $u_N(x, t)$, $v_N(x, t) \in X_N$, i.e.

$$u_N(x,t) = \sum_{l=-N/2}^{N/2-1} \hat{u}_l(t) \Phi_l(x), v_N(x,t) = \sum_{l=-N/2}^{N/2-1} \hat{v}_l(t) \Phi_l(x), \tag{2.8}$$

such that

$$(v_N)_{tt} = (v_N)_{xx} - \alpha (v_N)_{xxxx} + \mathcal{P}_N f(v_N)_{xx} + \omega \mathcal{P}_N (|u_N|^2)_{xx}, x \in \Omega, t > 0. \tag{2.9}$$

Substituting (2.8) into (2.9) and noticing the orthogonality of the basis functions in X_N, for $w \in \mathbb{R}$ and when t is near $t_n (n = 0, 1, \ldots)$, we obtain

$$\frac{d^2}{dw^2} \hat{v}_l(t_n + w) + \xi_l^2 \hat{v}_l(t_n + w) + \mu_l^2 (\hat{F}_l^n(w) + \omega \hat{G}_l^n(w)) = 0, \tag{2.10}$$

where $\xi_l = |\mu_l| \sqrt{1 + \alpha \mu_l^2}$, $\hat{F}_l^n(w) = (\widehat{f(v_N)})_l (t_n + w)$ and $\hat{G}_l^n(w) = (\widehat{|u_N|^2})_l (t_n + w)$.

Using the variation-of-constants formula [16], the general solution of above ODE is

$$\hat{v}_l(t_n+w)=cos(\xi_l w)\hat{v}_l(t_n)+\frac{sin(\xi_l w)}{\xi_l}\hat{v}_l'(t_n)-\frac{\mu_l^2}{\xi_l}\int_0^w(\hat{F}_l^n(s)+\omega\hat{G}_l^n(s))sin\big(\xi_l(w-s)\big)ds,\ n\geq 0. \tag{2.11}$$

Differentiating (2.11) with respect to w, we obtain

$$\hat{v}_l'(t_n+w)=\ cos(\xi_l w)\hat{v}_l'(t_n)-\xi_l sin(\xi_l w)\hat{v}_l(t_n)-\mu_l^2\textstyle\int_0^w(\hat{F}_l^n(s)+\omega\hat{G}_l^n(s))cos\big(\xi_l(w-s)\big)ds,\ n\geq 0. \tag{2.12}$$

For $n\geq 1$, choosing $w=\pm\tau$ in (2.11) and (2.12), then we obtain the following recursion relationship

$$\hat{v}_l(t_{n+1})=2cos(\xi_l\tau)\hat{v}_l(t_n)-\hat{v}_l(t_{n-1})-\frac{\mu_l^2}{\xi_l}\int_0^\tau\Big(\hat{F}_l^n(s)+\hat{F}_l^n(-s)+\omega(\hat{G}_l^n(s)+\hat{G}_l^n(-s))\Big)sin\big(\xi_l(\tau-s)\big)ds \tag{2.13}$$

and

$$\hat{v}_l'(t_{n+1})=\ \hat{v}_l'(t_{n-1})-2\xi_l sin(\xi_l\tau)\hat{v}_l(t_n)-\mu_l^2\textstyle\int_0^\tau\Big(\hat{F}_l^n(s)+\hat{F}_l^n(-s)+\omega(\hat{G}_l^n(s)+\hat{G}_l^n(-s))\Big)cos\big(\xi_l(\tau-s)\big)ds. \tag{2.14}$$

In order to design an explicit scheme, we adopt the Gautschi-type quadrature [16–18] with $A(s)\in C[0,\tau]$ and $0\neq\delta\in\mathbb{R}$:

$$\int_0^\tau A(s)sin(\delta(\tau-s))ds\approx A(0)\int_0^\tau sin(\delta(\tau-s))ds=\frac{A(0)}{\delta}(1-cos(\delta\tau)), \tag{2.15}$$

$$\int_0^\tau A(s)cos(\delta(\tau-s))ds\approx A(0)\int_0^\tau cos(\delta(\tau-s))ds=\frac{A(0)}{\delta}sin(\delta\tau) \tag{2.16}$$

to approximate all the integrals in (2.13) and (2.14).

Let $v_N^n(x)$ and $\dot{v}_N^n(x)$ be the approximations of $v(x,t_n)$ and $v_t(x,t_n)$, respectively. Then the details of exponential wave integrator Fourier spectral (EWI-FS) for Boussinesq-like equation is organized as follows:

$$v_N^n(x)=\sum_{l=-N/2}^{N/2-1}\hat{v}_l^n\Phi_l(x),\ \dot{v}_N^n(x)=\sum_{l=-N/2}^{N/2-1}\widehat{(\dot{v})}_l^n\Phi_l(x),\ n\geq 0, \tag{2.17}$$

where, for $n\geq 1$,

$$\hat{v}_l^{n+1}=2cos(\xi_l\tau)\hat{v}_l^n-\hat{v}_l^{n-1}-\frac{2\mu_l^2}{\xi_l^2}\Big(\hat{F}_l^n(0)+\omega\hat{G}_l^n(0)\Big)(1-cos(\xi_l\tau)), \tag{2.18}$$

$$\widehat{(\dot{v})}_l^{n+1}=\widehat{(\dot{v})}_l^{n-1}-2\xi_l sin(\xi_l\tau)\hat{v}_l^n-\frac{2\mu_l^2}{\xi_l}\Big(\hat{F}_l^n(0)+\omega\hat{G}_l^n(0)\Big)sin(\xi_l\tau). \tag{2.19}$$

Considering the initial condition (2.4), we have

$$\hat{u}_l^0=\widehat{(u^{(0)})}_l,\ \hat{v}_l^0=\widehat{(v^{(0)})}_l,\ \widehat{(\dot{v})}_l^0=\widehat{(v^{(1)})}_l. \tag{2.20}$$

In order to evaluate $\hat{v}_l^1$ and $\widehat{\dot{v}}_l^1$, using Taylor's expansion, we have

$$\hat{v}_l^1=\hat{v}_l^0+\tau\widehat{(\dot{v})}_l^0-\frac{\tau^2}{2}\Big(\xi_l^2\hat{v}_l^{(0)}+\mu_l^2(\widehat{f(v^{(0)})})_l+\omega\mu_l^2(\widehat{|u^{(0)}|^2})_l\Big), \tag{2.21}$$

$$\widehat{(\dot{v})}_l^1=\widehat{(\dot{v})}_l^0-\tau\Big(\xi_l^2\hat{v}_l^{(0)}+\mu_l^2(\widehat{f(v^{(0)})})_l+\omega\mu_l^2(\widehat{|u^{(0)}|^2})_l\Big). \tag{2.22}$$

In fact, above procedure is not suitable in practice due to the difficulty in computing the Fourier coefficients in (2.17)–(2.22) via the integration formula given in (2.6). By approximating the integrals in (2.17)–(2.22) by a quadrature rule on the grids $\{x_j\}_{j=0}^{N-1}$, we present an efficient implementation by using interpolation stated in (2.6) rather than the projection (integration).

Let v_j^n and $\dot{v}_j^n$ be the approximations of $v(x_j,t_n)$ and $v_t(x_j,t_n)$, respectively. Define

$$v_j^n=\sum_{l=-N/2}^{N/2-1}\tilde{v}_l^n\Phi_l(x_j),\ \dot{v}_j^n(x)=\sum_{l=-N/2}^{N/2-1}\widetilde{(\dot{v})}_l^n\Phi_l(x_j). \tag{2.23}$$

Then an exponential wave integrator Fourier pseudospectral (EWI-FP) method for Boussinesq equation reads as follows:

$$\tilde{v}_l^{n+1}=2cos(\xi_l\tau)\tilde{v}_l^n-\tilde{v}_l^{n-1}-\tfrac{2\mu_l^2}{\xi_l^2}\Big(\tilde{\mathcal{F}}_l^n+\omega\tilde{\mathcal{G}}_l^n\Big)(1-cos(\xi_l\tau)), \tag{2.24}$$

$$\widetilde{(\dot{v})}_l^{n+1}=\widetilde{(\dot{v})}_l^{n-1}-2\xi_l sin(\xi_l\tau)\tilde{v}_l^n-\tfrac{2\mu_l^2}{\xi_l}\Big(\tilde{\mathcal{F}}_l^n+\omega\tilde{\mathcal{G}}_l^n\Big)sin(\xi_l\tau), \tag{2.25}$$

$$\tilde{u}_l^0=\widetilde{(u^{(0)})}_l,\ \tilde{v}_l^0=\widetilde{(v^{(0)})}_l,\ \tilde{v}_l^1=\tilde{v}_l^0+\tau\widetilde{(\dot{v})}_l^0-\tfrac{\tau^2}{2}\Big(\xi_l^2\tilde{v}_l^0+\mu_l^2(\tilde{\mathcal{F}}_l^0+\omega\tilde{\mathcal{G}}_l^0)\Big), \tag{2.26}$$

$$\widetilde{(\dot{v})}_l^0=\widetilde{(v^{(1)})}_l,\ \widetilde{(\dot{v})}_l^1=\widetilde{(\dot{v})}_l^0-\tau\Big(\xi_l^2\tilde{v}_l^0+\mu_l^2(\tilde{\mathcal{F}}_l^0+\omega\tilde{\mathcal{G}}_l^0)\Big), \tag{2.27}$$

where $\mathcal{F}_j^n=f(v_j^n)$ and $\mathcal{G}_j^n=|u_j^n|^2$.

2.2. Time-splitting spectral method for Schrödinger-like equation

The basic idea of the time-splitting method for the nonlinear equations is to decompose a problem into linear and nonlinear subproblems on each time step. Considering the Strang splitting scheme [7,8,33] for Schrödinger-like equation (2.1), we can split it in the following sequential subproblems

$$\begin{cases} iu_t + \frac{\gamma}{2}u_{xx} = 0, \\ iu_t - \xi uv = 0, \qquad t \in [t_n, t_{n+1}]. \\ iu_t + \frac{\gamma}{2}u_{xx} = 0, \end{cases} \tag{2.28}$$

For the linear subproblem (2.28), we discretize it in space by Fourier spectral method as follows

$$i\frac{d}{dt}\hat{u}_l(t) = \frac{\gamma\mu_l^2}{2}\hat{u}_l(t), t \in [t_n, t_{n+1}], \tag{2.29}$$

then (2.29) can be solved exactly as

$$\hat{u}_l(t) = \hat{u}_l(t_n)e^{-\frac{i\gamma\mu_l^2}{2}(t-t_n)}, t \in [t_n, t_{n+1}]. \tag{2.30}$$

For the nonlinear subproblem in (2.28), we have

$$i\frac{du(x,t)}{u(x,t)} = \xi v(x,t)dt, t \in [t_n, t_{n+1}]. \tag{2.31}$$

Integrating (2.31) from t_n to t_{n+1}, and then approximating the integral on $[t_n, t_{n+1}]$ via trapezoidal rule, we obtain

$$u(x, t_{n+1}) = u(x, t_n)e^{-0.5i\xi(v(x,t_n)+v(x,t_{n+1}))}. \tag{2.32}$$

Based on (2.30) and (2.32), the time-splitting spectral (TSSP) method for solving (2.28), from t_n to t_{n+1} with $n = 0, 1, \ldots,$ is given as follows:

$$u_j^* = \sum_{l=-N/2}^{N/2-1} e^{i\mu_l(x_j-a)}\tilde{u}_l^n e^{-0.5i\gamma\mu_l^2\tau}, \tag{2.33}$$

$$u_j^{**} = u_j^* e^{-0.5i\xi(v_j^n+v_j^{n+1})}, \tag{2.34}$$

$$\tilde{u}_l^{n+1} = \frac{1}{N}\sum_{j=0}^{N-1} e^{-i\mu_l(x_j-a)}u_j^{**}e^{-0.5i\gamma\mu_l^2\tau}, \tag{2.35}$$

where v_j^{n+1} is evaluated by (2.24), i.e. $v_j^{n+1} = \sum_{l=-N/2}^{N/2-1}\tilde{v}_l^{n+1}e^{i\mu_l(x_j-a)}$.

Theorem 1. *The discretizations (2.33)–(2.35) for Schödinger-like equation posses the following property:*

$$h\sum_{j=0}^{N-1}|u_j^{n+1}|^2 = h\sum_{j=0}^{N-1}|u_j^n|^2, n \geq 0.$$

Proof. Noticing the identities

$$\sum_{j=0}^{N-1} e^{i\mu_l(x_j-a)} = \begin{cases} N, & l = 0, \\ 0, & l \neq 0, \end{cases} \sum_{l=-N/2}^{N/2-1} e^{i\mu_l(x_j-a)} = \begin{cases} N, & j = 0, \\ 0, & j \neq 0, \end{cases}$$

and Parserval's identity

$$\sum_{l=-N/2}^{N/2-1}|\tilde{u}_j^n|^2 = \frac{1}{N}\sum_{j=0}^{N-1}|u_j^n|^2,$$

thus from (2.33)–(2.35), we have

$$\begin{aligned} h\sum_{j=0}^{N-1}|u_j^{n+1}|^2 &= Nh\sum_{l=-N/2}^{N/2-1}|\tilde{u}_l^{n+1}|^2 = \frac{h}{N}\sum_{l=-N/2}^{N/2-1}\left|\sum_{j=0}^{N-1}e^{-i\mu_l(x_j-a)}u_j^{**}e^{-0.5i\gamma\mu_l^2\tau}\right|^2 \\ &= \frac{h}{N}\sum_{l=-N/2}^{N/2-1}\left|\sum_{j=0}^{N-1}e^{-i\mu_l(x_j-a)}u_j^{**}\right|^2 = \frac{h}{N}\sum_{l=-N/2}^{N/2-1}\left|\sum_{j=0}^{N-1}e^{-i\mu_l(x_j-a)}u_j^*e^{-0.5i\xi(v_j^n+v_j^{n+1})}\right|^2 \\ &= h\sum_{j=0}^{N-1}|u_j^*e^{-0.5i\xi(v_j^n+v_j^{n+1})}|^2 = h\sum_{j=0}^{N-1}\left|\sum_{l=-N/2}^{N/2-1}e^{i\mu_l(x_j-a)}\tilde{u}_l^n e^{-0.5i\gamma\mu_l^2\tau}\right|^2 \end{aligned}$$

$$= Nh\sum_{l=-N/2}^{N/2-1}|\tilde{u}_l^n e^{-0.5i\gamma\mu_l^2\tau}|^2 = Nh\sum_{l=-N/2}^{N/2-1}|\tilde{u}_l^n|^2 = h\sum_{j=0}^{N-1}|u_j^n|^2,$$

and the proof is completed. □

Remark 1. Theorem 1 implies that TS-EWI-FP method preserves the total mass in discrete level rigorously. As the author in [44] has mentioned that "it would be very challenging to propose a conservative EWI", thus, we do not expect that TS-EWI-FP method conserves the total energy in discrete level. According to Parserval's identity and (2.7), the total mass and energy can be discretized as

$$Q^n = Nh\sum_{l=-N/2}^{N/2-1}|\tilde{u}_l^n|^2 \tag{2.36}$$

and

$$E^n = Nh\sum_{l=-N/2}^{N/2-1}|\tilde{v}_l^n|^2 + Nh\tilde{\mathcal{K}}_0^n + Nh\sum_{l=-N/2}^{N/2-1}\left(\mu_l^2(\frac{2\omega\gamma}{\xi}|\tilde{u}_l^n|^2+\alpha|\tilde{v}_l^n|^2)+\frac{|\widetilde{(\dot{v})}_l^n|^2}{\mu_l^2}\right), \tag{2.37}$$

where $\mathcal{K}_j^n = 2F(v_j^n)+2\omega v_j^n|u_j^n|^2$ for $0\le j\le N-1$ and $n\ge 0$.

Remark 2. In this paper, we use Fourier pseudospertral method in the case of periodic boundary conditions. We remark here that corresponding sine pseudospectral can be established in a same way for homogenous Dirichlet boundary conditions.

3. TS-EWI-FP method for 2D SBq system

We consider 2D SBq system in a finite domain $\Omega=(a,b)\times(c,d)$ with periodic boundary conditions. Choosing $h_1 := (b-a)/N, h_2 := (d-c)/K$ with N and K are even positive integers, and denote grid points $(x_j, y_k, t_n) := (a+jh_1, c+kh_2, n\tau)$ for $0\le j\le N$, $0\le k\le K$ and $n\ge 0$.

Similar to Section 2.2, the TSSP scheme for the 2D Schrödinger-like equation is given as follows:

$$u_{jk}^* = \sum_{l=-N/2}^{N/2-1}\sum_{m=-K/2}^{K/2-1} e^{i\mu_l(x_j-a)}e^{i\nu_m(y_k-c)}\tilde{u}_{lm}^n e^{-0.5i\gamma(\mu_l^2+\nu_m^2)\tau}, \tag{3.1}$$

$$u_{jk}^{**} = u_{jk}^* e^{-0.5i\xi(v_{jk}^n+v_{jk}^{n+1})}, \tag{3.2}$$

$$\tilde{u}_{lm}^{n+1} = \frac{1}{NK}\sum_{j=0}^{N-1}\sum_{k=0}^{K-1} e^{-i\mu_l(x_j-a)}e^{-i\nu_m(y_k-c)}u_{jk}^{**}e^{-0.5i\gamma(\mu_l^2+\nu_m^2)\tau}, \tag{3.3}$$

where $\mu_l = \frac{2\pi l}{(b-a)}$, $\nu_m = \frac{2\pi m}{(d-c)}$, $-N/2\le j\le N/2-1$, $-K/2\le m\le K/2-1$. Here, u_{jk}^n represents the approximations of $u(x_j,\ y_k,\ t_n)$, $\tilde{u}_{lm}^n = \frac{1}{NK}\sum_{j=0}^{N-1}\sum_{k=0}^{K-1} u_{jk}^n e^{-i\mu_l(x_j-a)}e^{-i\nu_k(y_k-c)}$.

Next, we shall introduce the corresponding EWI-FP method for $2D$-Boussinesq-like equation. Let v_{jk}^n and $\dot{v}_{jk}^n$ be the approximations of $v(x_j,\ y_k,\ t_n)$ and $v_t(x_j,\ y_k,\ t_n)$, respectively. Define

$$v_{jk}^n = \sum_{l=-N/2}^{N/2-1}\sum_{m=-K/2}^{K/2-1}\tilde{v}_{lm}^n e^{i\mu_l(x_j-a)}e^{i\nu_m(y_k-c)},\ \dot{v}_{jk}^n = \sum_{l=-N/2}^{N/2-1}\sum_{m=-K/2}^{K/2-1}\widetilde{(\dot{v})}_{lm}^n e^{i\mu_l(x_j-a)}e^{i\nu_m(y_k-c)}.$$

Then EWI-FP for $2D$-Boussinesq-like equation is provided as follows:

$$\begin{aligned}
\tilde{v}_{lm}^{n+1} &= 2cos(\eta_{lm}\tau)\tilde{v}_{lm}^n - \tilde{v}_{lm}^{n-1} - \frac{2\gamma_{lm}^2}{\eta_{lm}^2}\left(\tilde{\mathcal{F}}_{lm}^n+\omega\tilde{\mathcal{G}}_{lm}^n\right)(1-cos(\eta_{lm}\tau)),\\
\widetilde{(\dot{v})}_{lm}^{n+1} &= \widetilde{(\dot{v})}_{lm}^{n-1} - 2\eta_{lm}sin(\eta_{lm}\tau)\tilde{v}_{lm}^n - \frac{2\gamma_{lm}^2}{\eta_{lm}}\left(\tilde{\mathcal{F}}_{lm}^n+\omega\tilde{\mathcal{G}}_{lm}^n\right)sin(\eta_{lm}\tau),\\
\tilde{u}_{lm}^0 &= \widetilde{(u^{(0)})}_{lm},\ \tilde{v}_{lm}^0 = \widetilde{(v^{(0)})}_{lm},\ \tilde{v}_{lm}^1 = \tilde{v}_{lm}^0 + \tau\widetilde{(\dot{v})}_{lm}^0 - \frac{\tau^2}{2}\left(\eta_{lm}^2\tilde{v}_{lm}^0+\gamma_{lm}^2(\tilde{\mathcal{F}}_{lm}^0+\omega\tilde{\mathcal{G}}_{lm}^0)\right),\\
\widetilde{(\dot{v})}_{lm}^0 &= \widetilde{(v^{(1)})}_{lm},\ \widetilde{(\dot{v})}_{lm}^1 = \widetilde{(\dot{v})}_{lm}^0 - \tau\left(\eta_{lm}^2\tilde{v}_{lm}^0+\gamma_{lm}^2(\tilde{\mathcal{F}}_{lm}^0+\omega\tilde{\mathcal{G}}_{lm}^0)\right),
\end{aligned}$$

where $\eta_{lm} = \gamma_{lm}\sqrt{1+\alpha\gamma_{lm}^2}$, $\gamma_{lm} = \sqrt{\mu_l^2+\nu_m^2}$, $\mathcal{F}_{jk}^n = f(v_{jk}^n)$ and $\mathcal{G}_{jk}^n = |u_{jk}^n|^2$.

Theorem 2. *The discretizations TSSP (3.1)-(3.3) for 2D Schödinger-like equation posses the following properties:*

$$Q^{n+1} = Q^n, n\ge 0,$$

where $Q^n = h_1h_2\sum_{j=0}^{N-1}\sum_{k=0}^{K-1}|u_{jk}^n|^2$.

Proof. From the Parserval's identity

$$\sum_{l=-N/2}^{N/2-1}\sum_{m=-K/2}^{K/2-1}|\widetilde{u}_{lm}^n|^2 = \frac{1}{NK}\sum_{j=0}^{N-1}\sum_{k=0}^{K-1}|u_{jk}^n|^2$$

and (3.1)–(3.3), we have

$$\begin{aligned}
Q^{n+1} &= NKh_1h_2\sum_{l=-N/2}^{N/2-1}\sum_{m=-K/2}^{K/2-1}|\widetilde{u}_{lm}^{n+1}|^2\\
&= \frac{h_1h_2}{NK}\sum_{l=-N/2}^{N/2-1}\sum_{m=-K/2}^{K/2-1}\left|\sum_{j=0}^{N-1}\sum_{k=0}^{K-1}e^{-i\mu_l(x_j-a)}e^{-i\nu_m(y_k-c)}u_{jk}^{**}e^{-0.5i\gamma(\mu_l^2+\nu_m^2)\tau}\right|^2\\
&= \frac{h_1h_2}{NK}\sum_{l=-N/2}^{N/2-1}\sum_{m=-K/2}^{K/2-1}\left|\sum_{j=0}^{N-1}\sum_{k=0}^{K-1}e^{-i\mu_l(x_j-a)}e^{-i\nu_m(y_k-c)}u_{jk}^{**}\right|^2\\
&= \frac{h_1h_2}{NK}\sum_{l=-N/2}^{N/2-1}\sum_{m=-K/2}^{K/2-1}\left|\sum_{j=0}^{N-1}\sum_{k=0}^{K-1}e^{-i\mu_l(x_j-a)}e^{-i\nu_m(y_k-c)}u_{jk}^{*}e^{-0.5i\xi(v_{jk}^n+v_{jk}^{n+1})}\right|^2\\
&= h_1h_2\sum_{j=0}^{N-1}\sum_{k=0}^{K-1}|u_{jk}^*e^{-0.5i\xi(v_{jk}^n+v_{jk}^{n+1})}|^2 = h_1h_2\sum_{j=0}^{N-1}\sum_{k=0}^{K-1}|u_{jk}^*|^2\\
&= h_1h_2\sum_{j=0}^{N-1}\sum_{k=0}^{K-1}\left|\sum_{l=-N/2}^{N/2-1}\sum_{m=-K/2}^{K/2-1}e^{i\mu_l(x_j-a)}e^{i\nu_m(y_k-c)}\widetilde{u}_{lm}^n e^{-0.5i\gamma(\mu_l^2+\nu_m^2)\tau}\right|^2\\
&= NKh_1h_2\sum_{l=-N/2}^{N/2-1}\sum_{m=-K/2}^{K/2-1}|\widetilde{u}_{lm}^n e^{-0.5i\gamma(\mu_l^2+\nu_m^2)\tau}|^2 = NKh_1h_2\sum_{l=-N/2}^{N/2-1}\sum_{m=-K/2}^{K/2-1}|\widetilde{u}_{lm}^n|^2 = Q^n.
\end{aligned}$$

Here, we used the identities

$$\sum_{j=0}^{N-1}\sum_{k=0}^{K-1}e^{i\mu_l(x_j-a)}e^{i\nu_m(y_k-c)} = \begin{cases}NK, & l=m=0,\\ 0, & \text{others,}\end{cases}$$

and

$$\sum_{l=-N/2}^{N/2-1}\sum_{k=-K/2}^{K/2-1}e^{i\mu_l(x_j-a)}e^{i\nu_m(y_k-c)} = \begin{cases}NK, & j=k=0,\\ 0, & \text{others.}\end{cases}$$

□

Accordingly, the mass $Q(t_n)$ and energy $E(t_n)$ in (1.2) and (1.3) can be discreted as

$$Q^n = NKh_1h_2\sum_{l=-N/2}^{N/2-1}\sum_{m=-K/2}^{K/2-1}|\widetilde{u}_{lm}^n|^2 \tag{3.4}$$

and

$$\begin{aligned}
E^n = {}& NKh_1h_2\sum_{l=-N/2}^{N/2-1}\sum_{m=-K/2}^{K/2-1}|\widetilde{v}_{lm}^n|^2 + NKh_1h_2\widetilde{\mathcal{M}}_{00}^n + NKh_1h_2\sum_{l=-N/2}^{N/2-1}\sum_{m=-K/2}^{K/2-1}\frac{|\widetilde{(\dot{v})}_{lm}^n|^2}{\gamma_{lm}^2}\\
&+ NKh_1h_2\sum_{l=-N/2}^{N/2-1}\sum_{k=-K/2}^{K/2-1}\gamma_{lm}^2\left(\frac{2\omega\gamma}{\xi}|\widetilde{u}_{lm}^n|^2+\alpha|\widetilde{v}_{lm}^n|^2\right),
\end{aligned} \tag{3.5}$$

where $\mathcal{M}_{jk}^n = 2f(v_{jk}^n) + 2\omega v_{jk}^n|u_{jk}^n|^2$.

4. Numerical results

In this section, we carry out some numerical experiments to test the performance of TS-EWI-FP method for SBq system in 1D and 2D. When $d=1$ and $f(v)=\theta v^2$, the SBq system admits the solitary-wave solutions:

Table 1
Spatial discretization error of TS-EWI-FP for different h at time $t = 1$ under $\tau = 1/10,000$.

h		1	1/2	1/4
Example 1	L_2^n	1.1815e-0	2.7526e-3	3.6502e-8
	L_∞^n	6.6201e-1	1.1146e-3	1.8768e-8
Example 2	L_2^n	1.5327e-3	1.4299e-7	1.1726e-9
	L_∞^n	8.5741e-4	2.8596e-8	3.5501e-10
Example 3	L_2^n	8.8377e-1	1.2824e-2	1.9729e-7
	L_∞^n	4.0391e-1	5.0017e-3	5.8704e-8

Case 1: If $\gamma\xi d_1 = 2b_1(3\gamma\theta - \alpha\xi)$ and $3\alpha\xi \neq \gamma\theta$ and $4\alpha b_1 \neq \gamma d_1$,

$$\begin{cases} u(x,t) = \pm\frac{6b_1}{\xi}\sqrt{\frac{\gamma\theta-\alpha\xi}{\gamma\omega}}sech(\mu\zeta)tanh(\mu\zeta)e^{i(\frac{M}{2\gamma}x+\delta t)}, \\ v(x,t) = -\frac{6b_1}{\xi}sech^2(\mu\zeta), x\in\mathbb{R}, t\geq 0. \end{cases} \tag{4.1}$$

Case 2: If $3\alpha\xi = \gamma\theta$ and $4\alpha b_1 \neq \gamma d_1$,

$$\begin{cases} u(x,t) = \sqrt{\frac{6\alpha b_1}{\gamma^2\theta\omega}(\gamma d_1 - 4\alpha b_1)}sech(\mu\zeta)e^{i(\frac{M}{2\gamma}x+\delta t)}, \\ v(x,t) = -\frac{2b_1}{\xi}sech^2(\mu\zeta), x\in\mathbb{R}, t\geq 0. \end{cases} \tag{4.2}$$

Case 3: If $\gamma d_1 + 2\alpha b_1 = 0$ and $\theta = 0$,

$$\begin{cases} u(x,t) = \sqrt{\frac{18b_1 d_1}{\omega\xi}}sech(\mu\zeta)tanh(\mu\zeta)e^{i(\frac{M}{2\gamma}x+\delta t)}, \\ v(x,t) = -\frac{6b_1}{\xi}sech^2(\mu\zeta), x\in\mathbb{R}, t\geq 0. \end{cases} \tag{4.3}$$

Here $b_1 = \delta + \frac{M^2}{4\gamma}$, $d_1 = 1 - M^2$, $\mu = \sqrt{\frac{b_1}{\gamma}}$, $\zeta = x - Mt$ and M, δ are free parameters. In this paper, we provide following three types of solitary-wave solutions related to Case 1-Case 3, respectively.

Example 1. Let $\gamma = 1$, $\xi = 1$, $\alpha = \frac{2}{3}$, $\theta = \frac{1}{9}$, $\omega = -\frac{1}{2}$ and $M = \sqrt{\frac{22}{15}}$ and $\delta = \frac{1}{3}$.

Example 2. Let $\gamma = 1$, $\xi = 1$, $\alpha = \frac{1}{2}$, $\theta = \frac{3}{2}$, $\omega = \frac{1}{12}$ and $M = \frac{1}{\sqrt{3}}$ and $\delta = \frac{1}{5}$.

Example 3. Let $\gamma = 1$, $\xi = -6$, $\alpha = 1$, $\theta = 0$, $\omega = 2$ and $M = \sqrt{3}$ and $\delta = \frac{1}{4}$.

In the numerical experiments of Examples 1–3, we always take $\Omega = [-64, 64]$. To quantify the errors of numerical solutions, we introduce following error functions

$$L_2^n = \sqrt{h\sum_{j=0}^{N-1}|u_j^n - u(x_j,t_n)|^2} + \sqrt{h\sum_{j=0}^{N-1}|v_j^n - v(x_j,t_n)|^2}$$

and

$$L_\infty^n = \max_{0\leq j\leq N-1}|u_j^n - u(x_j,t_n)| + \max_{0\leq j\leq N-1}|v_j^n - v(x_j,t_n)|.$$

To test the spatial discretization error, we take a small time step $\tau = 1/10,000$ such that the temporal discretization error is negligible compared to the spatial discretization error, and the errors are tabulated in Table 1.

To verify the accuracy and efficiency of TS-EWI-FP, we compare TS-EWI-FP method with previous methods. It should be pointed that TSFP [2] and Scheme I [30] are fully implicit while TS-EWI-FP method is an explicit scheme, thus, TS-EWI-FP is expected to be more efficient than other methods. In our implementation, the iteration operation continues until the following conditions are satisfied

$$\max_{0\leq j\leq N-1}|u_j^{n(s+1)} - u_j^{n(s)}| \leq 10^{-12}, \max_{0\leq j\leq N-1}|v_j^{n(s+1)} - v_j^{n(s)}| \leq 10^{-12}.$$

Tables 2–4 indicate that TS-EWI-FP method is more accurate and efficient than the mentioned methods.

For the temporal discretization error, we take a small $h = 1/4$ such that the space discretization error is negligible compared to the discretization error in time, and the errors are reported in Tables 5–7. Tables 5–7 demonstrate that the temporal discretization precision of TS-EWI-FP is more accurate than TSFP and Scheme I.

In order to measure fluctuated amplification of the discretization conservation quantities, we define relative errors of them via the following formulations

$$R_Q^n = |(Q^n - Q^0)/Q^0|, R_E^n = |(E^n - E^0)/E^0|.$$

Table 2
Comparison of maximum norm error and computational time for Example 1 with different h at $t = 1$ under $\tau = 1/10,000$.

h	1 L^n_∞/CPU time (s)	1/2 L^n_∞/CPU time (s)	1/4 L^n_∞/CPU time (s)
TSFP[2] ($\beta = \frac{1}{2}$)	6.6201e-1/148.5(s)	1.1146e-3/626.4(s)	6.6233e-8/2419.4(s)
Scheme I [30]	1.2201e-0/164.1(s)	5.2059e-2/428.8(s)	2.8647e-3/726.7(s)
TS-EWI-FP	6.6201e-1/18.8(s)	1.1146e-3/59.6(s)	1.8768e-8/323.3(s)

Table 3
Comparison of maximum norm error and computational time for Example 2 with different h at $t = 1$ under $\tau = 1/10,000$.

h	1	1/2	1/4
TSFP[2] ($\beta = \frac{1}{2}$)	8.5741e-4/127.8(s)	2.8660e-8/314.5(s)	1.6693e-9/1791.6(s)
Scheme I [30]	9.5384e-3/137.1(s)	4.8946e-4/215.3(s)	3.2353e-5/547.1(s)
TS-EWI-FP	8.5741e-4/17.1(s)	2.8596e-8/58.2(s)	3.5501e-10/338.6(s)

Table 4
Comparison of maximum norm error and computational time for Example 3 with different h at $t = 1$ under $\tau = 1/10,000$.

h	1	1/2	1/4
TSFP[2] ($\beta = \frac{1}{2}$)	4.0391e-1/135.5(s)	5.0017e-3/288.8(s)	1.1729e-7/1879.4(s)
Scheme I [30]	7.5288e-1/172.7(s)	7.2543e-2/333.4(s)	3.8150e-3/872.8(s)
TS-EWI-FP	4.0391e-1/14.6(s)	5.0017e-3/52.3(s)	5.8704e-8/286.6(s)

Table 5
Comparison of temporal discretization error and computational time for Example 1 with different τ at $t = 1$ under $h = 1/4$.

τ	1/16	1/32	1/64
TSFP[2] ($\beta = \frac{1}{2}$)	2.6350e-2/7.8(s)	6.6101e-3/12.5(s)	1.6573e-3/20.7(s)
Scheme I [30]	1.0656e-2/4.8(s)	4.4113e-3/8.9(s)	3.1175e-3/15.6(s)
TS-EWI-FP	6.6150e-3/0.5(s)	1.6429e-3/1.1(s)	4.0963e-4/2.2(s)

Table 6
Comparison of temporal discretization error and computational time for Example 2 with different τ at $t = 1$ under $h = 1/4$.

τ	1/16	1/32	1/64
TSFP[2] ($\beta = \frac{1}{2}$)	1.0443e-4/8.6(s)	2.6392e-5/12.5(s)	6.6347e-6/20.7(s)
Scheme I [30]	6.8382e-5/3.4(s)	3.8254e-5/4.7(s)	3.2462e-5/10.1(s)
TS-EWI-FP	9.9217e-5/0.5(s)	2.4974e-5/1.1(s)	6.2677e-6/1.9(s)

Table 7
Comparison of temporal discretization error and computational time for Example 3 with different τ at $t = 1$ under $h = 1/4$.

τ	1/16	1/32	1/64
TSFP[2] ($\beta = \frac{1}{2}$)	3.0290e-2/2.1(s)	7.3769e-3/4.2(s)	1.8408e-3/8.3(s)
Scheme I [30]	9.6215e-3/7.8(s)	4.6829e-3/8.9(s)	3.9923e-3/15.1(s)
TS-EWI-FP	5.2334e-3/0.4(s)	1.1888e-3/0.8(s)	2.9247e-4/1.8(s)

Table 8
Conservation properties test of Example 3 with different (h, τ).

(h, τ)		$t = 0$	$t = 5$	$t = 10$
(1/2, 1/50)	Q^n	15.6176442753612	15.6176163598460	15.6175886542631
	R^n_Q	0	1.78743443710e-6	3.56142687448e-6
	E^n	90.8848715484718	90.8898643268920	90.8898641164655
	R^n_E	0	5.49351980707e-5	5.493288276246e-5
(1/2, 1/100)	Q^n	15.6176442753612	15.6176301850418	15.61761632075927
	R^n_Q	0	9.02205167534e-7	1.789937167300e-6
	E^n	90.8848715484718	90.8861276360173	90.88620339173646
	R^n_E	0	1.38206449990e-5	1.465417997394e-5

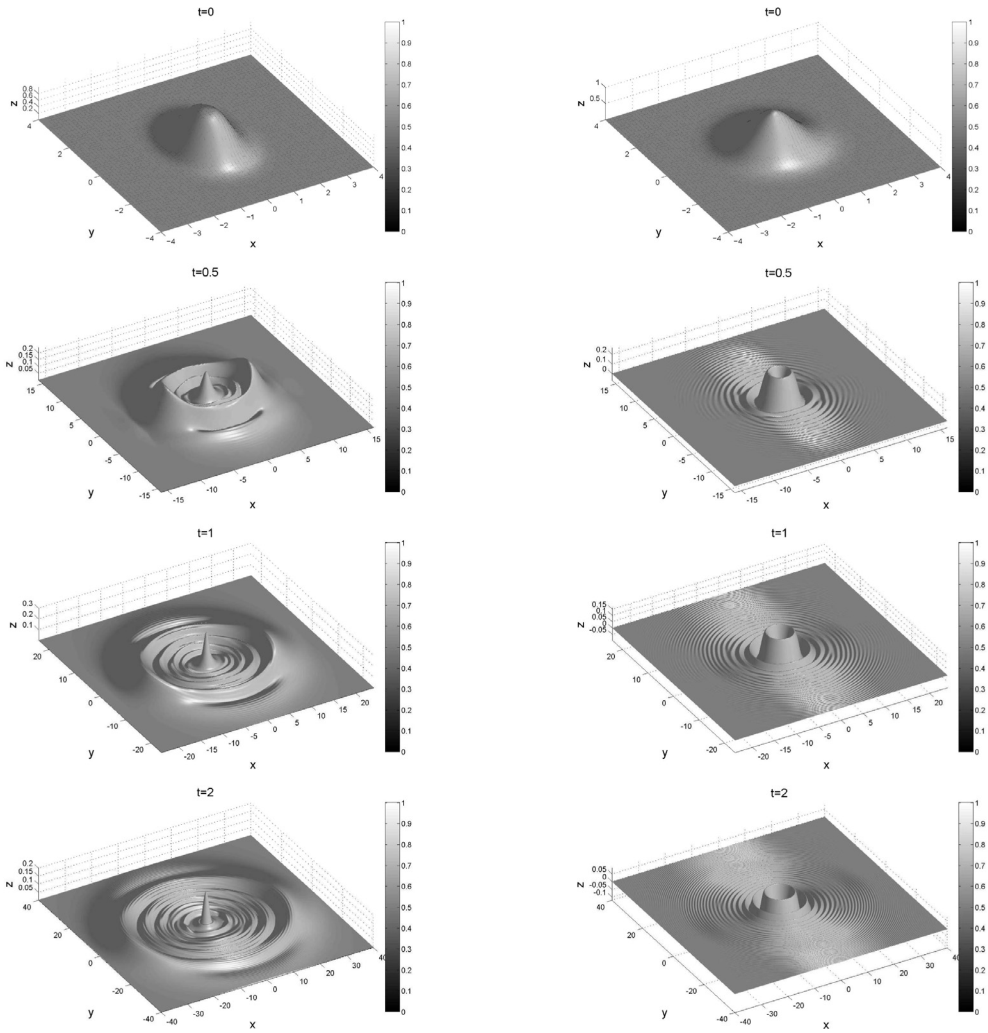

Fig. 1. Surface plots of $|u(x, y, t)|$ (left column) and $v(x, y, t)$ (right column) in Example 4 at different times with $h_1 = h_2 = 1/8$ and $\tau = 1/800$.

Table 9
Stability analysis: $e^n = \frac{\|u(\cdot,t_n)-u^n\|_{l^2}}{\|u(\cdot,t_n)\|_{l^2}} + \frac{\|v(\cdot,t_n)-v^n\|_{l^2}}{\|v(\cdot,t_n)\|_{l^2}}$ is computed at $t = 10$.

h		Example 1	Example 2	Example 3
1/2	τ	1/4	1/2	1/4
	e^n	1.7926e-1	6.5237e-2	8.1628e-1
1/4	τ	1/8	1/4	1/8
	e^n	3.5480e-2	1.5550e-2	1.1744e-1
1/8	τ	1/16	1/8	1/16
	e^n	8.7515e-3	3.8687e-3	1.6478e-2

To examine the conservation properties, we have computed the total mass, total energy and the relative errors of Example 3 in Table 8.

From Table 8, we can see that TS-EWI-FP conserves the total mass very well, which validates the conclusion in Theorem 1. Although TS-EWI-FP is not proved to conserve the total energy, Table 8 demonstrates that the smaller temporal step τ is, the less fluctuated amplification of the discretization energy.

From Table 9, we can see that the stability constraint of TS-EWI-FP is weaker, it requires $\tau = O(h)$.

Example 4. Dynamics of SBq system in 2D, we choose $f(v) = sin(v),\ \gamma = \alpha = 1$ and $\xi = \omega = \frac{1}{10}$ in (1.1). The initial data are taken as

$$u^{(0)}(x, y) = \frac{2}{e^{x^2+2y^2} + e^{-(x^2+2y^2)}} e^{5i/cosh(\sqrt{4x^2+y^2})},$$

$$v^{(0)}(x, y) = e^{-(x^2+y^2)},\ v^{(1)}(x, y) = \frac{1}{2} e^{-(x^2+y^2)},\ (x, y) \in (-64, 64)^2.$$

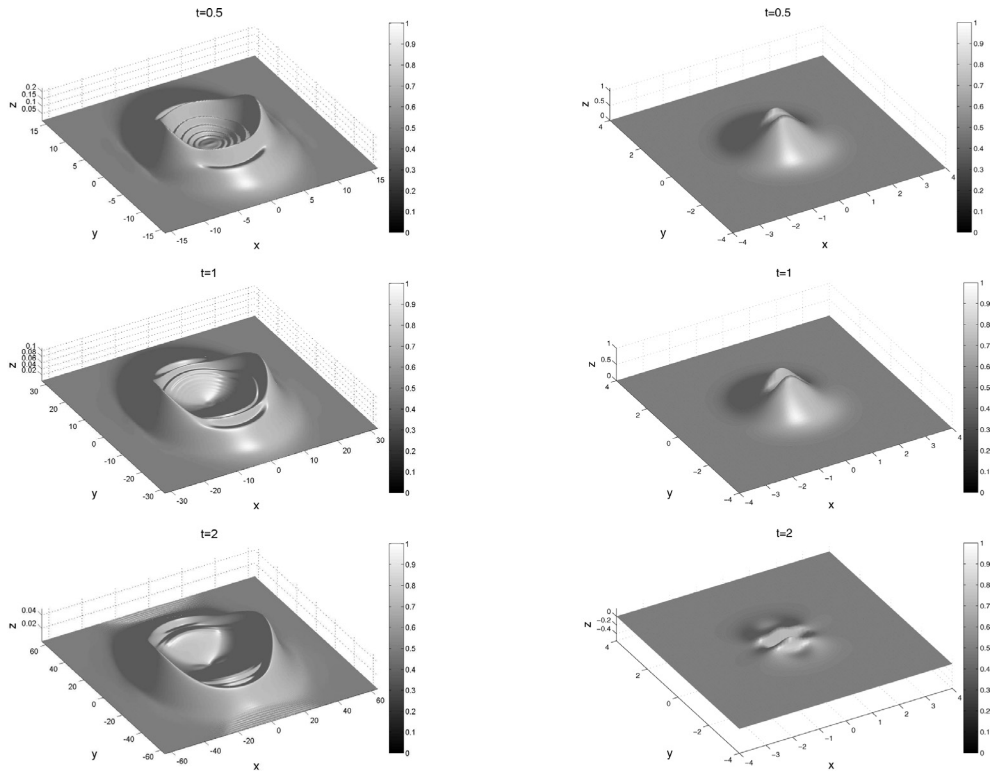

Fig. 2. Surface plots of $|u(x, y, t)|$ (left column) and $v(x, y, t)$ (right column) in Example 5 at different times with $h_1 = h_2 = 1/8$ and $\tau = 1/800$.

Table 10
Conservation quantities test of Example 4 with different (h_1, h_2, τ).

(h_1, h_2, τ)		$t = 0$	$t = 1$	$t = 2$
(1/4, 1/4, 1/400)	Q^n	2.22144310016832	2.22144310017107	2.22144310017096
	R_Q^n	0	1.2408428220e-12	1.1906653533e-12
	E^n	−3.269153177e+04	−3.253210898e+04	−3.252885945e+04
	R_E^n	0	0.00487657762907	0.00497597717413
(1/4, 1/4, 1/800)	Q^n	2.22144310016832	2.22144310016966	2.22144310017050
	R_Q^n	0	6.0432863721e-13	9.8155924866e-13
	E^n	−3.269153177e+04	−3.265676981e+04	−3.265445933e+04
	R_E^n	0	0.00106333213172	0.00113400749530

Fig. 1 shows the surface plots of $|u|$ (left column) and v (right column) at different times. Conservation quantities test of Example 4 is reported in Table 10. Since Zakharov system is a special case of SBq system, to make a comparison between Zakharov system and SBq system, we also utilize TS-EWI-FP to solve 2D Zakharov system in Example 5.

Example 5. Dynamics of Zakharov system in 2D, we choose $f(v) = 0,\ \gamma = 1, \alpha = 0$ and $\xi = \omega = \frac{1}{10}$ in (1.1). The initial data, computational domain and temporal step are similar to Example 4. The surface plots of $|u|$ and v are listed in Fig. 2.

Figs. 1 and 2 demonstrate that the efficiency and high resolution of TS-EWI-FP, which could be used to study the dynamics behavior of SBq system in high space dimensions.

5. Conclusion

We formulate an efficient and accurate TS-EWI-FP method for computing SBq system. Compared with previous methods in [1,2,23,25,30,43,46], TS-EWI-FP is fully explicit and efficient due to the fast Fourier transform. The numerical results indicate that TS-EWI-FP method is more accurate than other mentioned methods, and conserves the total mass in discrete level very well. In addition, we utilize TS-EWI-FP method to solve SBq system in 2D, the numerical results demonstrate the efficiency and high resolution of our method for studying the dynamics of SBq system in high space dimensions.

Acknowledgements

We, authors, express our deep gratitude to editor-in-chief, his staff and anonymous referees for their invaluable contributions to a better content and careful reading of the manuscript.

References

[1] Bai DM, Zhang LM. The quadratic B-spline finite element method for the coupled Schrödinger-Boussinesq equations. Inter J Comput Math 2011;88:1714–29.
[2] Bai DM, Wang JL. The time-splitting Fourier spectral method for the coupled Schrödinger-Boussinesq equations. Commun nonlinear Sci Numer Simulat 2012;17:1201–10.
[3] Bai DM, Zhang LM. Numerical studies on a novel split-step quadratic B-spline finite element method for the coupled Schrödinger-KDV equations. Commun nonlinear Sci Numer Simulat 2011;16:1263–73.
[4] Bao WZ, Dong XC. Analysis and comparison of numerical methods for the Klein-Gordon equation in the nonrelativistic limit regime. Numer Math 2012;120:189–229.
[5] Bao WZ, Dong XC, Zhao XF. An exponential wave integrator sine pseudospectral method for the Klein-Gordon-Zakharov system. SIAM J Sci Comput 2013;35:A2903–27.
[6] Bao WZ, Cai YY. Uniform and optimal error estimates of an exponential wave integrator sine pseudospectral method for the nonlinear Schrödinger equation with wave operator. SIAM J Numer Anal 2014;52:1103–27.
[7] Bao WZ, Jin S, Markowich PA. On time-splitting spectral approxomations for the Schrödinger equation in the semiclassical regime. J Comput Phys 2002;175:487–524.
[8] Bao WZ, Yang L. Efficient and accurate numerical methods for the Klein-Gordon-Schrödinger equations. J Comput Phys 2007;225:1863–93.
[9] Bao WZ, Sun FF, Wei GW. Numerical methods for the generalized Zakharov system. J Comput Phys 2003;190:201–28.
[10] Bilige S, Chaolu ST, Wang XM. Application of the extended simplest equation method to the coupled Schrödinger-Boussinesq equation. Appl Math Comput 2013;224:517–23.
[11] Chang QS, Guo BL, Jiang H. Finite difference method for generalized Zakharov equations. Math Comput 1995;64:537–53.
[12] Dehghan M, Taleei A. A compact split-step finite difference method for solving the nonlinear Schrödinger equations with constant and variable coefficients. Comput Phys Commun 2010;181:43–51.
[13] Dong XC. A trigonometric integrator pseudospectral discretization for the N-coupled nonlinear Klein–Gordon equations. Numer Algor 2013;62:325–36.
[14] Dong XC. Stability and convergence of trigonometric integrator pseudospectral discretization for N-coupled nonlinear Klein–Gordon equations. Appl Math Comput 2014;232:752–65.
[15] Farah LG, Pastor A. On the periodic Schrödinger-Boussinesq system. J Math Anal 2010;368:330–49.
[16] Gautschi W. Numerical integration of ordinary differential equations based on trigonometric polynomials. Numer Math 1961;3:381–97.
[17] Grimm V. A note on the Gautschi-type method for oscillatory second-order differential equations. Numer Math 2005;102:61–6.
[18] Grimm V. On error bounds for the Gautschi-type exponential wave integrator applied to oscillatory second-order differential equations. Numer Math 2005;100:71–89.
[19] Guo BL. The global solution of the system of equations for complex Schrödinger field coupled with Boussinesq type self-consistent field. Acta Math Sinica 1983;26:295–306. (in Chinese)
[20] Guo BL, Chen FX. Finite dimensional behavior of global attractors for weakly damped nonlinear Schrödinger–Boussinesq equations. Phys D 1996;93:101–18.
[21] Guo BL, Du XY. The behavior of attractors for the weakly damped Schrödinger-Boussinesq equation. Commun Nonlinear Sci Numer Simulat 2001;6:54–60.
[22] Guo BL, Du XY. Existence of the periodic solution for the weakly damped Schrödinger-Boussinesq equation. J Math Anal Appl 2001;262:453–72.
[23] Guo BL, Chen GN. The convergence of Galerkin-Fourier method for equation of Schrödinger-Boussinesq field. J Comput Math 1984;2:344–55.
[24] Hon YV, Fan E. A seris of exact solutions for coupled Higgs field equation and coupled Schrödinger-Boussinesq equation. Nonlinear Anal 2009;71:3501–8.
[25] Huang LY, Jiao YD, Liang DM. Multi-sympletic scheme for the coupled Schrödinger-Boussinesq equations. Chin Phys B 2013;22:1–5.
[26] Jin S, Markowich PA, Zheng CX. Numerical simulation of a generalized Zakharov system. J Comput Phys 2004;201:376–95.
[27] Jin S, Zheng CX. A time-splitting spectral method for the generalized Zakharov system in multi-dimensions. J Sci Comput 2006;26:127–49.
[28] Kilicman A, Abazari R. Travelling wave solutions of the Schrödinger–Boussinesq system. Abst Appl Anal 2012;2012:1–11.
[29] Li YS, Chen QY. Finite dimensional global attractor for dissipative Schrödinger–Boussinesq equations. J Math Anal Appl 1997;205:107–32.
[30] Liao F, Zhang LM. Conservative compact finite difference scheme for the coupled Schrödinger–Boussinesq equation. Numer Methods Part Differ Eq 2016;32:1667–88.
[31] Rao NN. Exact sloutions of coupled scalar field equations. J Phys A Math General 1989;22:4813–25.
[32] Rao NN. Coupled scalar field equations for nonlinear wave modulations in dispersive media. Pramana J Pyhs 1991;46:161–202.
[33] Strang G. On the construction and comparison of difference schemes. SIAM J Numer Anal 1968;5:505–17.
[34] Taleei A, Dehghan M. Time-splitting pseudo-spectral domain decomposition method for the soliton solutions of the one-and multi-dimensional nonlinear Schrödinger equations. Comput Phys Commun 2014;185:1515–28.
[35] Wang HQ. Numerical studies on the split-step finite difference method for nonlinear Schrödinger equations. Appl Math Comput 2005;170:17–35.
[36] Wang SS, Zhang LM. Split-step orthogonal spline collocation methods for nonlinear Schrödinger equations in one,two, and three dimensions. Appl Math Comput 2011;218:1903–16.
[37] Wang SS, Wang TC, Zhang LM. Numerical computations for n-coupled nonlinear Schrödinger equations by split step spectral methods. Appl Math Comput 2013;222:438–52.
[38] Weideman JAC, Herbst BM. Split-step methods for the solution of the nonlinear Schrödinger equation. SIAM J Numer Anal 1986;23:485–507.
[39] Xia YH, Xu Y, Shu CW. Local discontinuous Galerkin methods for the generalized Zakharov system. J Comput Phys 2010;229:1238–59.
[40] Yajima N, Satsuma J. Soliton solutions in a diatomic lattice system. Prog Theor Phys 1979;62:370–8.
[41] Yao RX, Li ZB. Exact explict solutions of the nonlinear Schrödinger equation coupled to the Boussinesq equation. Acta Math Scientia 2003;23B:453–60.
[42] Zakharov VE. Collapse of Langmuir waves. Sov Phys JETP 1972;35:908–14.
[43] Zhang LM, Bai DM, Wang SS. Numerical analysis for a conservative difference scheme to solve the Schrödinger-Boussinesq equation. J Comput Appl Math 2011;235:4899–915.
[44] Zhao XF. On error estimates of an exponential wave integrator sine pseudospectral method for the Klein-Gordon–Zakharov system. Numer Methods Part Differ Eq 2016;32:266–91.
[45] Zhao XF. An exponential wave integrator pseudospectral method for the symmetric regularized-long-wave equation. J Comput Math 2016;34:49–69.
[46] Zheng JD, Xiang XM. The finite element analysis for the equation system coupling the complex Schrödinger and real Boussinesq fields. Math Numer Sinica 1987;5:133–43. (in Chinese)